Renewable Energy 196 (2022) 1366–1375

Contents lists available at ScienceDirect

Renewable Energy

journal homepage: www.elsevier.com/locate/renene

Sizing of energy storage systems for ramp rate control of photovoltaic strings

Kari Lappalainen [a,*], Seppo Valkealahti [a]

[a] Tampere University, Electrical Engineering Unit, 33720, Tampere, Finland

ARTICLE INFO

Keywords:
Energy storage sizing
Energy storage system
Photovoltaic power generation
Photovoltaic string
Power variation
Ramp rate control

ABSTRACT

In this article, a comprehensive study on the sizing of energy storage systems (ESS) for ramp rate (RR) control of photovoltaic (PV) strings is presented. The effects of RR limit and inverter sizing, including their combined effect, on the sizing of the ESS are herein studied systematically for the first time. The study is based on 38 days of current–voltage curve measurements of a PV string of 23 PV modules. The results show that the daily irradiance profile has a crucial effect on the ESS power and energy requirements. It was found that an ESS power rating of 60% of the PV string nominal power is adequate to smooth almost all detected PV power ramps even with strict RR limits. With a typical DC/AC power ratio of 1.5, about 1.0 h of energy storage capacity is needed at the nominal power of the PV string to smooth all PV power ramps. The results illustrate that the set RR limit and the inverter sizing are important factors for sizing the ESS for PV RR control. Moreover, the results indicate that the needed ESS power capacity can be considerably reduced by smoothing the fastest upward power ramps by power curtailment.

1. Introduction

The power output of photovoltaic (PV) power plants is highly variable due to fast irradiance fluctuations, which are mainly caused by overpassing cloud shadows. As the share of grid-connected PV power production capacity increases, the grids will be more vulnerable to power imbalance, thus endangering the security of the whole power system. Utilisation of variable renewable energy sources, like PV, in distribution grids is limited by the restricted local generation hosting capacity of the grids. Output power variations of the variable renewable energy sources can be smoothed using energy storage systems (ESS), enabling grid integration of larger shares of renewable energy generation. Moreover, storage capacity can be utilised when the power production of variable renewable energy sources exceeds the power demand. Some transmission system operators have already set limits for power ramp rates (RR) of grid-connected PV power plants [1]. For instance, the Puerto Rico Electric Power Authority has limited power RRs to 10 %/min of rated power [2]. However, variations that are multiple times faster exist in the output power of PV power plants. Power variations of up to 70 %/min were reported in Ref. [3] for a 9.5 MWp PV plant. In small-scale PV systems, power variations can be even faster: power variations of over 40 %/s were measured for a 3.2 kWp PV string [4]. In Ref. [5], a review of mitigating methods of PV power fluctuations is presented. Compliance with RR requirements has typically been achieved using ESSs or by power output curtailment. Nevertheless, the application of power curtailment is limited to upward power ramps.

The ESS power requirement needed to buffer all downward PV power ramps is determined by the largest PV power RRs. Output power variation of PV systems has been studied comprehensively in recent years. A simulation study of power variations of various PV array sizes and electrical configurations was presented in Ref. [6], and power variations of large-scale PV power plants were studied by simulations in Ref. [7] and based on experimental measurements in Refs. [3,8]. Smoothing of power fluctuations with increasing PV array size has been studied in several articles, e.g. in Refs. [9,10]. In addition to increasing PV array size, PV power fluctuations can be smoothed by geographical dispersion [11,12]. Thus, compliance with RR requirements is challenging, especially for small-scale PV power plants, such as individual PV strings. Because increasing ESS power and energy capacity increases the cost of the ESS, sizing the ESS needs to be balanced against benefits in RR mitigation. Reliable estimation of the largest expected PV power RRs provides an opportunity to size the ESS optimally, decreasing RR mitigation costs. Methods for estimation of the largest expected PV power RRs were presented in Refs. [13,14]. Due to the speed of PV

* Corresponding author.
E-mail addresses: kari.lappalainen@tuni.fi (K. Lappalainen), seppo.valkealahti@tuni.fi (S. Valkealahti).

https://doi.org/10.1016/j.renene.2022.07.069
Received 10 May 2022; Received in revised form 7 July 2022; Accepted 14 July 2022
Available online 19 July 2022

Nomenclature

E_{ESS}	energy stored in the ESS (Wh)
$E_{ESS,\ min}$	minimum energy stored in the ESS (Wh)
I	current (A)
$I_{MPP,\ STC}$	PV string maximum power point current at STC (A)
$I_{SC,\ STC}$	PV string short-circuit current at STC (A)
P_{ESS}	power fed to the ESS (W)
$P_{ESS,\ charge}$	charging power of the ESS (W)
$P_{ESS,\ dicharge}$	discharging power of the ESS (W)
P_{grid}	power fed to the grid (W)
$P_{grid,\ max}$	maximum power fed to the grid (W)
P_{inv}	power fed to the inverter (W)
$P_{MPP,\ STC}$	PV string maximum power point power at STC (W)
P_{PV}	PV string power (W)
$P_{PV,\ nom}$	nominal power of the PV string (W)
U	voltage (V)
$U_{MPP,\ STC}$	PV string maximum power point voltage at STC (V)
$U_{OC,\ STC}$	PV string open-circuit voltage at STC (V)

Abbreviations

AC	alternating current
DC	direct current
ESS	energy storage system
PV	photovoltaic
MPP	maximum power point
OC	open-circuit
RR	ramp rate
RR_{grid}	ramp rate of the power fed to the grid
RR_{lim}	ramp rate limit
SC	short-circuit
STC	standard test conditions

power variations, fast-responding energy storage technologies like batteries, capacitors and superconductive magnetic ESSs are best suited for PV power RR mitigation. An overview of various energy storage technologies is given, for example, in Ref. [15].

PV generators are usually oversized with respect to their inverters, meaning that the generator nominal DC power exceeds the inverter nominal AC power [16]. Oversizing of a PV generator restricts the generator power to the inverter nominal power during high irradiance conditions. If the PV generator produces more power than the inverter maximum power, the inverter will operate in power-limiting mode, moving the operating point to higher voltages to limit the current and power of the inverter. PV power variations occurring with powers higher than the inverter maximum power are not transmitted to AC power. In addition to energy losses, operating in power-limiting mode may also decrease the efficiency and lifetime of the inverter: the efficiency of some inverters decreases [17] and the capacitor lifetime shortens [18] under high DC side voltages. The optimal inverter sizing depends on many factors, such as inverter characteristics and irradiance conditions [19]. It is recommended in Ref. [20] that the DC/AC power ratio, i.e. the ratio of the nominal DC power of the PV generator to the inverter nominal AC power, should be from 1.1 to 1.7. The results of [21,22] show that the DC/AC ratio should be less than 1.0 to avoid all power curtailment. The effects of inverter sizing on the optimal operating point of PV generators have been studied in Ref. [23]. It was found that, if the aim is to minimise energy losses, the expected maximum clear-sky irradiance should be the basis for inverter sizing so that the PV generator would be in power-limiting mode only during cloud enhancement.

Several methods have been presented for PV power smoothing. These methods can be divided into filter-based methods, moving average and exponential smoothing based methods, RR-based methods, and model predictive control methods [24,25]. The control method used affects the sizing and lifetime of the ESS. A comparison of RR control algorithms for PV systems equipped with ESSs is presented in Ref. [26]. Sizing of an ESS for PV, wind and wave power, with regard to hourly smoothing and annual levelling was studied in Ref. [27]. In some studies, like [28], ESS control algorithms smoothing upward power ramps by limiting the inverter power are presented. These algorithms aim to reduce the use of the ESS at the cost of power curtailment losses. This kind of power curtailment is simple to implement for upward power ramps. However, in order to apply power curtailment during downward power fluctuations, accurate power forecasting is needed. If a downward power fluctuation is detected early enough, it is possible to reduce the inverter power at the set RR before the downward power ramp, i.e. the arrival of a shadow. Several ESS control algorithms utilising PV power forecasting have been proposed recently [29,30]. A review of PV power forecasting methods is given in Ref. [31]. AC and DC bus interconnections of ESSs in PV power plants controlled by an RR-based method were compared in Ref. [32] utilising simulated PV powers.

Several ESS control methods have been proposed in recent years for PV power smoothing. However, the effects of factors affecting the control and sizing of ESSs, such as the applied RR limit and inverter sizing, have not been studied comprehensively. In Ref. [28], equations to calculate the energy capacity needed to absorb the worst upward and downward fluctuations were presented, taking into account the applied RR limit. However, the effects of the RR limit on the sizing of ESSs were not studied. In Ref. [33], smoothing of short-term PV power fluctuations was studied by controlling the ESS with an RR-based method with seven RR limits. The power and energy requirements of the ESS were found to decrease with loosening the RR limit. In Ref. [34], two novel techniques were proposed for reducing the size of the ESS, combining an RR-based control method and inverter power curtailment. The techniques were tested using 1 s power data from a 7.2 MWp PV plant with two DC/AC ratios. It was concluded that multiple decision factors arise when combining the ESS size-reduction techniques with power curtailment and inverter sizing. As far as we know, the combined effect of the RR limit and inverter sizing has not been studied earlier. To fill this knowledge gap, in this article, a comprehensive study on the sizing of ESSs for PV strings based on measured current–voltage (*I–U*) curves is presented. The effects of the RR limit and inverter sizing, including their combined effect, on the sizing of ESSs for RR control of PV strings are studied systematically for the first time. The RR limit was altered from 1 to 20 %/min and the DC/AC power ratio from 1.0 to 2.0. In total, over 2 million *I–U* curves measured over 38 days were analysed.

The main novelty of this study is that, for the first time, the effects of the RR limit and inverter sizing on the sizing of ESSs for RR control of PV strings are extensively studied based on actual PV string *I–U* curve measurements. In earlier studies [33,34], the effects of these factors have been illustrated using only a few example values for the factors. In this study, the effects of the RR limit and inverter sizing are studied systematically for the first time. Moreover, the present study is based on comprehensive experimental measurements performed with a high sampling frequency while some of the previous studies, e.g. Ref. [32], were based on simulated PV powers. The main objective of this study is to determine what requirements PV power variability imposes on the ESSs used for RR control of PV strings. The requirements studied include the ESS charge and discharge powers and the energy capacity needed to compensate for all PV power fluctuations exceeding the applied RR limit. Moreover, it is studied how large a share of produced energy is cycled through the ESS. The results of this study demonstrate that the set RR limit and inverter sizing, together with the daily irradiance profile, have a crucial effect on the ESS power and energy requirements, meaning that they should be considered carefully when sizing an ESS for

PV power RR control. Thus, the first comprehensive experimental study of the effects of the RR limit and inverter sizing on the sizing of the ESSs presented in this article is a worthwhile contribution to the current knowledge and provides valuable information for design and control of PV power plants equipped with ESSs. The results of this study are particularly relevant for design of PV power plants equipped with ESSs, including the sizing and control of the ESS and the sizing of the inverter.

The rest of the article is organised as follows. Section 2.1 introduces the measurement data used. In Section 2.2, the RR control strategy used is introduced, and its operation is illustrated. The results when the inverter is sized to match up with the PV string nominal power are presented in Section 3.1. The effects of inverter sizing on ESS sizing are then discussed in Section 3.2. In Section 4, the results and their significance are further discussed. Finally, the conclusions are presented in Section 5.

2. Methods and data

2.1. Measurement data

This study is based on measured *I–U* curves of a PV string of 23 series-connected PV modules of the PV power research plant at Tampere University [35]. The *I–U* curves were measured during 38 days in May, June, August and September 2021 and in April and May 2022. All the measurement days are listed in the Appendix. The measurement period of each day in April, May, June and August was 15 h, from 5:00 to 20:00 (UTC+2), i.e. all the daylight hours were analysed. In September, the measurement period was 13 h, from 6:00 to 19:00, due to shorter day-length. The layout scheme of the studied PV string is presented in Fig. 1. The PV string is composed of NAPS NP190GK modules consisting of 3 submodules of 18 polycrystalline silicon PV cells. Each submodule is protected by an anti-parallel-connected bypass diode. The nominal standard test conditions (STC) values of the string at the maximum power point (MPP), open-circuit (OC) and short-circuit (SC) are compiled in Table 1. Nine PV modules of the string are equipped with irradiance and temperature measurements at a sampling frequency of 10 Hz. The back-sheet temperature of the modules was measured by Pt100 temperature sensors and the irradiance incident on the modules

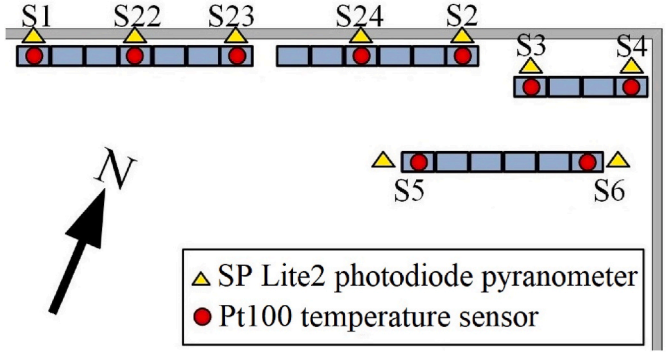

Fig. 1. Layout scheme of the studied PV string.

Table 1
Details of the studied PV string. The nominal STC values were calculated using the nominal STC values of NAPS NP190GK PV modules.

Parameter	Value
Number of modules	23
$P_{MPP,\ STC}$ (W)	4370
$U_{MPP,\ STC}$ (V)	593
$I_{MPP,\ STC}$ (A)	7.36
$U_{OC,\ STC}$ (V)	759
$I_{SC,\ STC}$ (A)	8.00

was measured by photodiode-based SP Lite2 pyranometers, installed at the same 45° tilt angle and 157° azimuth angle from north to east as the PV modules.

An *I–U* curve tracer was used to measure the *I–U* curve once per second during the measurement period of 558 h. The *I–U* curve, consisting of 4000 measurement points, was traced by loading the PV string with an adjustable resistance altering the output current of the string. Parallel connected IGBTs, which act as an electronic variable load, are gate controlled with a ramp signal for opening and closing channels of the transistors. The direction of the measurement sweep is from OC to SC. The voltage was measured by a LeCroy AP031 differential voltage probe and the current by a Tektronix TCP312A current probe with a Tektronix TCPA300 current probe amplifier. The *I–U* curves were pre-processed as follows. First, the points with identical measured voltage value were replaced with a single point by averaging their measured current values. Thereafter, clearly abnormal measurement points were removed. A point was considered to be clearly abnormal if its power differed from the power of the previous and next point by more than 1.3 times the mean power change between adjacent measurement points (previous and next nine points). Finally, the current and voltage measurements of each curve were smoothed separately using the smooth.m function in MATLAB. The use of the measured *I–U* curves instead of AC powers allows studying the technology-independent ESS requirements imposed by PV power variability without taking into account the non-idealities and losses related to MPP tracking, inverter, etc. In that way, the results are not as tied to a certain system. For the same reason, losses of the ESS were not considered. Moreover, the use of the measured *I–U* curves allows easy simulation of various DC/AC power ratios.

Fast variations existing in the output power of PV strings are illustrated in Fig. 2, where the behaviour of the measured *P–U* and *I–U* curves is presented during a fast irradiance transition. The largest change of the measured PV power in 1 s occurred between the second and third curve from the top, when the global MPP power decreased 1710 W, or 39.1% of the nominal MPP power. The change in the global

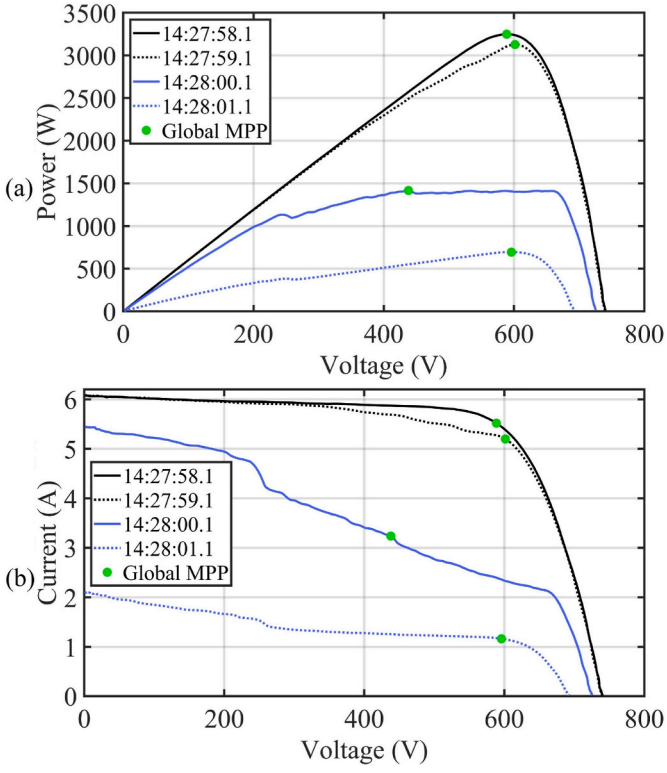

Fig. 2. Four consecutive power–voltage (a) and current–voltage (b) curves measured during a fast irradiance transition on September 3, 2021.

MPP power during the following second was 723 W, meaning that the PV power decreased 2433 W, or 55.7%, in just 2 s. The fastest increase of the global MPP power in 1 s during the measurement period of 558 h was 37.8%. These values are well in line with [4], where the maximum changes of power measured for two PV strings of 18 modules were 37.2% and 43.8% in a second. It can be seen in Fig. 2 that fast changes also occur in the voltage of the global MPP. Variation of the global MPP voltage has been studied, for example, in Ref. [4]. It is worth noting that Fig. 2 presents an extreme example of fast PV power variation, and in practise the fastest power ramps exist only infrequently. Since the largest PV power RRs determine the ESS power requirements, the daily irradiance profile is expected to have a major effect on the ESS power requirements.

2.2. Control strategy

The simulation model used, containing the PV string, ESS and inverter, is presented in Fig. 3. The power generated by the PV string P_{PV} equals the sum of the power fed to the inverter P_{inv} and the charging power of the ESS P_{ESS}, i.e. $P_{PV} = P_{inv} + P_{ESS}$. The measured MPP power of the PV string was used as the output power of the string, i.e. the PV string was assumed to operate at its MPP all the time. Inverter losses were not taken into account, meaning that the power fed to the inverter was equal to the power fed to the grid P_{grid}, i.e. $P_{inv} = P_{grid}$. The maximum power fed to the grid $P_{grid,\,max}$ was limited by the inverter sizing (DC/AC ratio) and can be expressed as

$$P_{grid,\,max} = \frac{P_{PV,\,nom}}{\text{DC/AC ratio}}, \tag{1}$$

where $P_{PV,\,nom}$ is the nominal power of the PV string, i.e. the PV string MPP power at STC. The DC/AC power ratio was changed between 1.0 and 2.0, and the cut power was fed to the ESS. The capacity of the ESS was not limited because the purpose of this study was to determine the size of the ESS needed to smooth all PV power ramps faster than the set RR limit.

The RR control of the PV system was implemented by an RR-based control strategy. RR of the power fed to the grid RR_{grid} was limited to comply with the set RR limit RR_{lim} so that

$$\left|RR_{grid}\right| \le RR_{lim}, \tag{2}$$

where RR_{grid} was calculated by dividing the change in the power fed to the grid between two consecutive time steps by their time difference. The RR limit compliance was achieved by storing enough energy in the ESS to smooth the power ramp at any time in the case of a sudden shutdown of the PV generator. Thus, the minimum energy stored in the ESS at each moment depended on the power fed to the grid at that moment, and can be expressed as

$$E_{ESS,\,min} = \frac{{P_{grid}}^2}{2RR_{lim}}. \tag{3}$$

To maximise the energy yield to the grid, the ESS energy level was kept as close to the minimum determined by Eq. (3) as possible by

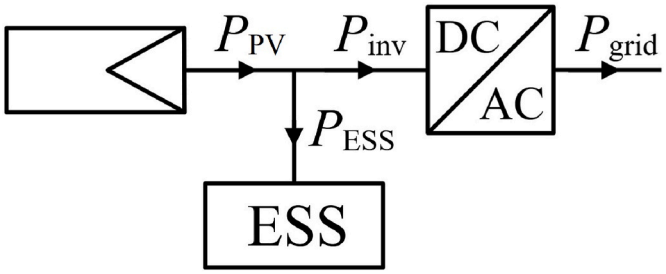

Fig. 3. Diagram of the PV system simulation model.

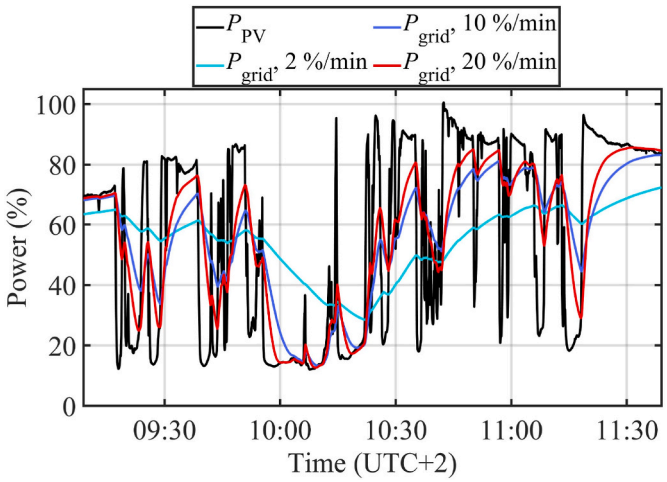

Fig. 4. Power of the PV string and the power fed to the grid with three different RR limits on the morning of June 9, 2021. The powers are with respect to the PV string nominal power.

discharging the ESS whenever possible. The RR limit was altered from 1 to 20 %/min of the nominal grid connection power $P_{grid,\,max}$.

The operation of the control strategy used is illustrated in Figs. 4 and 5. Fig. 4 shows the measured PV string power together with simulated powers fed to the grid with three different RR limits for a period of two and a half hours. How the ESS smooths the power fed to the grid compared to the highly fluctuating power output of the PV string is clearly visible in Fig. 4. Naturally, the smoothing is stronger as the RR limit is stricter. Fig. 5 provides a blow-up of Fig. 4 for 1 h of the ESS power together with the PV string power and the power fed to the grid when the RR limit was 10 %/min of $P_{grid,\,max}$. During this period, the required power capacity of the ESS was about half of the PV string nominal power $P_{PV,\,nom}$.

The methodology used does not take into account the losses and other nonidealities of real ESSs. A realistic consideration of charge–discharge cycling induced degradation, efficiency and response time of the ESSs would have made the simulation model much more complicated [36]. However, the methodology is suitable for determining the ESS requirements imposed by PV power variability, which is the main objective of this study. The aim of the study is especially to provide ESS technology-independent guidelines for the sizing of the ESSs for RR control of PV strings.

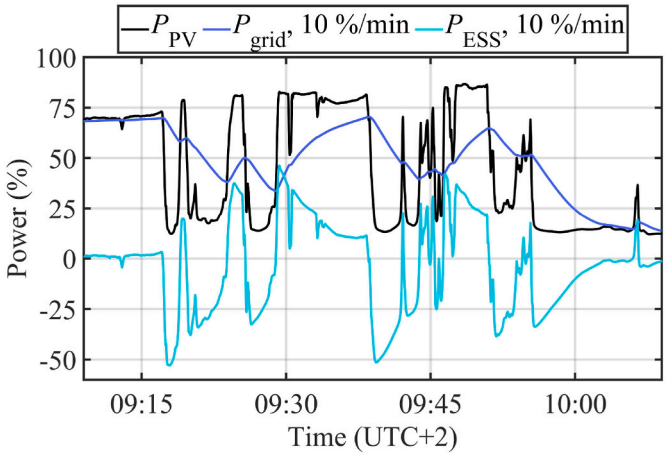

Fig. 5. Power of the PV string, the power fed to the grid and the power of the ESS with an RR limit of 10 %/min on the morning of June 9, 2021. The powers are with respect to the PV string nominal power.

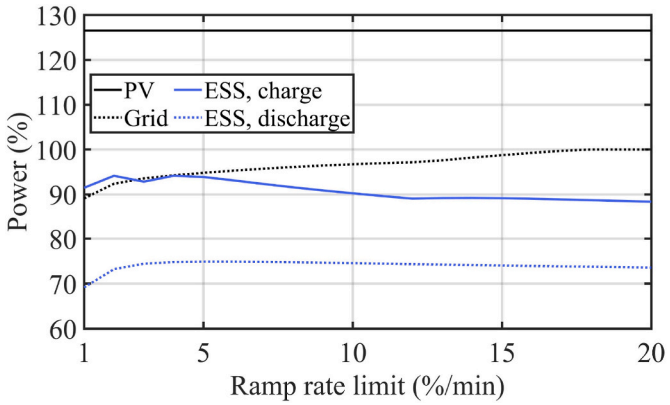

Fig. 6. The highest PV string power, power fed to the grid and the ESS power during the measurement period of 38 days as a function of the RR limit. The powers are with respect to the PV string nominal power.

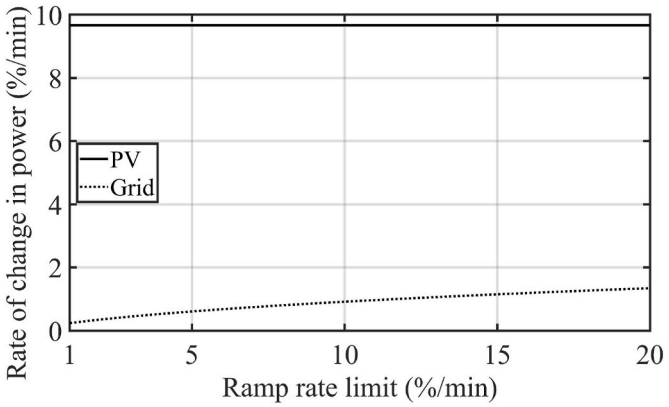

Fig. 7. Average rates of change in the PV power and the power fed to the grid during the measurement period of 38 days as a function of the RR limit. The powers are with respect to the PV string nominal power.

3. Results

The measured PV power is divided into the power fed to the grid and the charging power of the ESS utilising the control strategy introduced in Section 2.2 for the measurement period of 558 h. In Section 3.1, inverter size is selected to match the PV string nominal power. That is, DC/AC power ratio is 1.0, while the applied RR limit is varied. In Section 3.2, the study is extended to cover undersized inverters relative to the PV string nominal power. Both the DC/AC ratio and the RR limit are varied to study their combined effect on the ESS sizing.

3.1. Inverter sized to match the PV string nominal power

Fig. 6 presents the highest PV string power, the highest ESS charging and discharging power and the highest power fed to the grid during the measurement period as a function of the RR limit. The highest PV string power was almost 130% with respect to the nominal power, meaning that cloud enhancement effects have occurred during the measurement period [21]. Naturally, the highest PV power is independent of the RR limit. The highest power fed to the grid increased with the increasing RR limit. The highest ESS charging power was clearly higher than the highest ESS discharging power with all the studied RR limits. The reason for this is that the ESS discharge always started from the power fed to the grid, but the charging of the ESS also compensated for increases in the PV string power in the case of cloud enhancement effects, i.e. when the inverter limited the power fed to the grid. The highest ESS charging and discharging powers decreased slightly as the RR limit increased except at very strict RR limits. The maximum power requirement of the ESS does not seem to be very sensitive to the applied RR limit. The reason for this is that the power ramps which moving clouds cause for PV strings are mostly much faster than even the strictest RR limits [4]. The highest ESS power was also found to decrease with the increasing RR limit in Ref. [33]. That study considered larger PV power plants, and thus the decrease of ESS power requirement with the increasing RR limit was larger than presented in Fig. 6, becoming steeper with increasing plant size.

The average rates of change in the PV power and the power fed to the grid are presented in Fig. 7 as a function of the RR limit. The average rate of change in the PV power during the measurement period of 558 h was 9.7 %/min. The average rate of change in the power fed to the grid was clearly smaller, below 1.4 %/min, illustrating the efficiency of PV power RR smoothing. Naturally, the average rate of change in the power fed to the grid increased with the increasing RR limit because the RR limit determines the highest permitted rate of change in the power fed to the grid. With an RR limit of 1 %/min, the average rate of change in the power fed to the grid was about 24% of the RR limit. This ratio decreased with the increasing RR limit being about 7% with an RR limit of 20 %/min.

Fig. 8 presents the highest, average and lowest daily maximum power of the ESS as a function of the RR limit. The daily irradiance profile has a major effect on the ESS power requirements, as expected in Section 2.1. On clear-sky days, the ESS is mainly used for preparation for potential PV power fluctuations. Thus, the maximum ESS powers remain at low level. On the other hand, compensation for fast irradiance fluctuations that occur on partly cloudy days requires high power ratings of the ESS. The highest daily maximum ESS power was over 88% of the PV string nominal power for all the RR limits. On average, the highest daily maximum ESS power was a bit over 50% of the PV string nominal power. These findings are important, meaning that an ESS power rating of 60% of the PV string nominal power is high enough to smooth almost all PV power ramps, even with strict RR limits, while a power rating of 95% is needed to smooth even the rarely existing fastest PV power ramps. The highest daily ESS charging and discharging powers are compiled in Table A1 for an RR limit of 10 %/min.

Values for the highest, average and lowest daily maximum energy stored in the ESS are presented in Fig. 9 as a function of the RR limit. The stored energy is presented with respect to the PV string nominal power, meaning that a capacity of 1 h is equal to energy produced by the PV string at its nominal power in 1 h. The daily maximum energy stored in the ESS is the energy capacity of the ESS needed to smooth all the PV power RRs to comply with the set RR limit. On clear-sky days, maximum energy stored in the ESS is the energy needed to ramp down the highest power fed to the grid if the PV string is suddenly disconnected, as

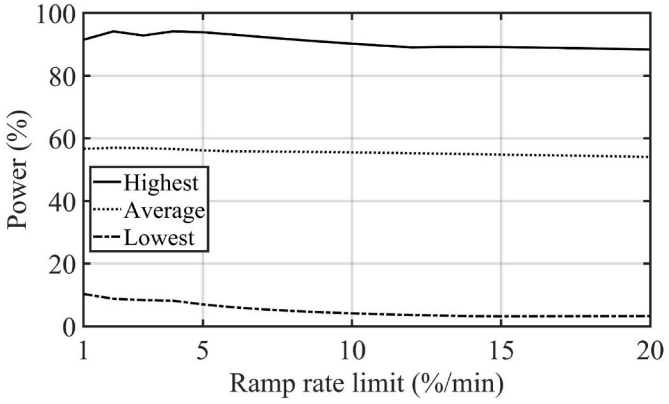

Fig. 8. The highest, average and lowest daily maximum power of the ESS as a function of the RR limit. The powers are with respect to the PV string nominal power.

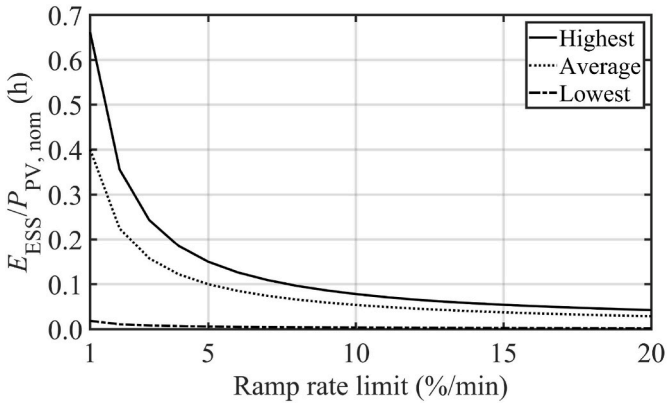

Fig. 9. The highest, average and lowest daily maximum energy stored in the ESS with respect to the PV string nominal power as a function of the RR limit.

determined by Eq. (3). The daily maximum energy stored in the ESS decreases sharply with the increasing RR limit, in line with the findings of [33]. The highest amount of energy stored in the ESS was 0.66 h at the nominal power of the PV string with an RR limit of 1 %/min, whereas it was only 0.08 h with an RR limit of 10 %/min. The daily maximum energies stored in the ESS are presented in the Appendix for an RR limit of 10 %/min.

Fig. 10 presents the relative cumulative frequencies of the amount of energy stored in the ESS, i.e. the needed energy capacity, for three different RR limits. Most of the time, only a small amount of energy was stored in the ESS. Half of the time the stored energy was less than 0.042, 0.006 and 0.003 h at the nominal power of the PV string for the RR limits of 1, 5 and 10 %/min, respectively. The amount of stored energy was over 0.05 h 48.5%, 25.6% and 10.1% of time for the RR limits of 1, 5 and 10 %/min, respectively.

The highest, average and lowest daily shares of produced energy cycled through the ESS are presented in Fig. 11 as a function of the RR limit. The shares of energy cycled through the ESS decreased with the increasing RR limit as the need to smooth slower PV power ramps decreased. On clear-sky days, the energy cycled through the ESS is approximately the energy needed to ramp down the power fed to the grid in case of sudden PV string disconnection. Depending on the applied RR limit, an average of 5%–15% of the energy produced per day was cycled through the ESS. On the day when the irradiance conditions varied the most, the share of energy cycled through the ESS was roughly twice that, from 14% to 29%. The results shown in Figs. 8, 9 and 11 illustrate what an enormous effect the daily irradiance conditions have on the power and energy capacity requirements of the ESS to smooth all PV power ramps. The daily shares of energy cycled through the ESS are compiled in Table A1 for an RR limit of 10 %/min.

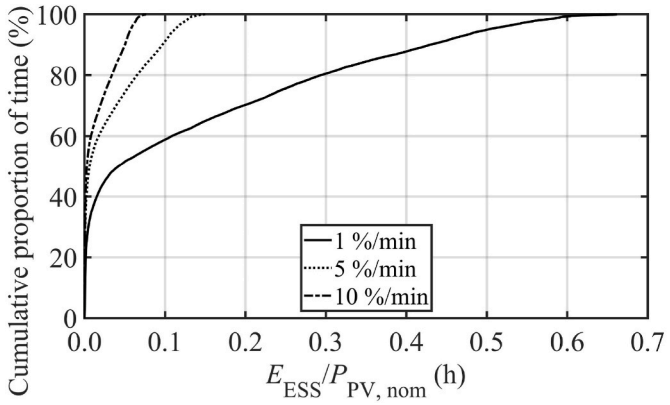

Fig. 10. Relative cumulative frequencies of the energy stored in the ESS with respect to the PV string nominal power for three different RR limits.

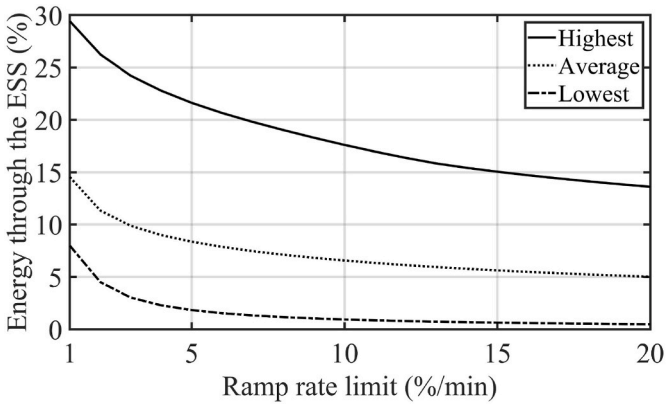

Fig. 11. The highest, average and lowest daily shares of energy cycled through the ESS as a function of the RR limit.

3.2. Undersized inverter relative to the PV string nominal power

The highest ESS discharging and charging powers during the measurement period are presented in Fig. 12 as a function of the DC/AC power ratio and RR limit. The highest ESS discharging and charging powers for a DC/AC ratio of 1.0 are also presented in Fig. 6. The highest discharging power decreased with increasing DC/AC ratio but was quite constant as a function of the RR limit at all the DC/AC ratios. The variation of the highest charging power with changing DC/AC ratio and RR limit is much smaller than the variation of the highest discharging power. The highest charging power was between 88.4% and 94.3% of the PV string nominal power for all combinations of the DC/AC ratio and RR limit, whereas the highest discharging power of the ESS was always below 76%. Fig. 12 confirms that the finding shown in Fig. 6 is generally valid, i.e. that the highest ESS charging powers are higher than the highest discharge powers for all DC/AC ratios. The reason for this is that the ESS

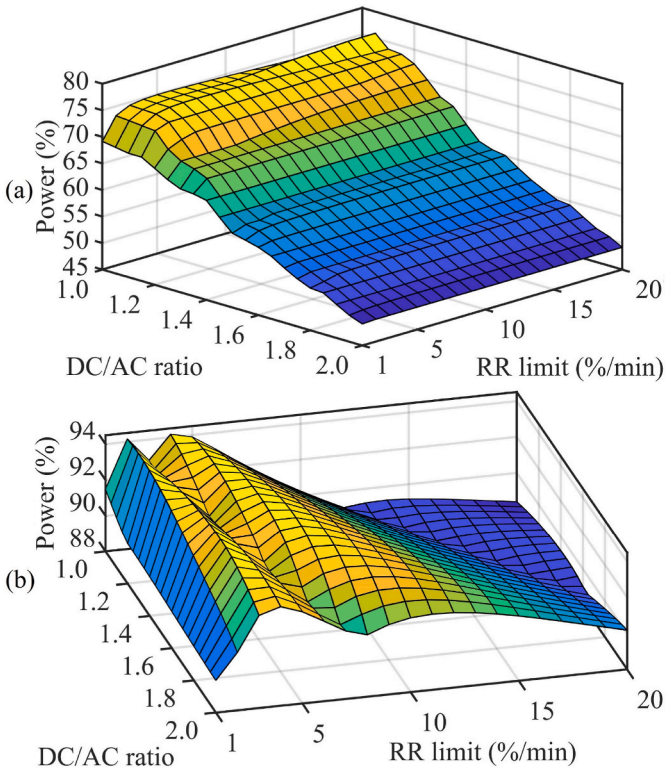

Fig. 12. The highest ESS discharging (a) and charging (b) powers as a function of the DC/AC ratio and the RR limit. The powers are with respect to the PV string nominal power.

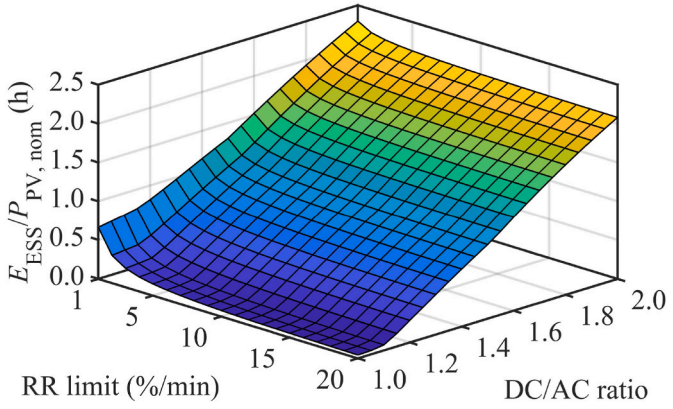

Fig. 13. The maximum energy stored in the ESS as a function of the RR limit and the DC/AC power ratio. The energy is with respect to the PV string nominal power.

discharge always started from the power fed to the grid, but the charging of the ESS also compensated for the increase in power in the case of cloud enhancement effects. This means that the ESS power capacity can be considerably reduced by curtaining the powers higher than the PV string nominal power without storing them to the ESS and, further, by smoothing the fastest upward power ramps by limiting the inverter power. Since the fastest power ramps exist only seldom, the associated power curtailment losses would be slight. This illustrates the potential for reducing ESS power capacity with ESS control algorithms smoothing the fastest upward power ramps by limiting the inverter power.

Fig. 13 shows the maximum energy stored in the ESS as a function of the RR limit and the DC/AC power ratio, i.e. the ESS energy capacity needed to comply with the set RR limit for the PV plant all the time. The maximum energy stored in the ESS with a DC/AC ratio of 1.0 is also presented in Fig. 9. The needed energy capacity increases strongly with the increasing DC/AC ratio. This is an expected result because cycling of the curtained power through the ESS increases with the increasing DC/AC ratio. The maximum energy stored in the ESS was more than 2.0 h at the PV string nominal power when the DC/AC ratio was 2.0, and with a typical DC/AC ratio of 1.5, it was about 1.0 h. One should also note that the needed ESS energy capacity increased only slightly when the DC/AC ratio increased from 1.0 to 1.2. This is due to the fact that the clear sky irradiance coming to PV modules in Tampere never reaches the STC irradiance of 1 kW/m^2, which means that the PV string will not produce its nominal power. The required energy capacity decreases as the RR limit increases with all the DC/AC ratios. The decrease is significant at strict RR limits below 5 %/min but rather modest at higher RR limits.

The share of energy cycled through the ESS during the measurement period is presented in Fig. 14 as a function of the RR limit and the DC/AC power ratio. It was found in Section 3.1 (Fig. 11) that the share of the produced energy cycled through the ESS decreases with the increasing RR limit. Fig. 14 confirms that finding to be valid for all DC/AC ratios. As expected, the share of energy cycled through the ESS increased with the increasing DC/AC ratio. With a typical DC/AC ratio of 1.5, from 12% to 19% of the energy produced by the PV string was cycled through the ESS. For a DC/AC ratio of 2.0, the share was from 23% to 28%. However, the energy cycled through the ESS increased only slightly as the DC/AC ratio increased from 1.0 to 1.2, because the clear sky irradiance coming to PV modules in Tampere never reaches 1 kW/m^2. Cycling a large share of produced energy through the ESS daily will accelerate charge–discharge cycling induced degradation and thus shorten the lifetime of the ESS. The results show the large effect of inverter sizing on ESS sizing. Based on the results, it is evident that the DC/AC ratio and the set RR limit should be carefully considered when determining the capacity for the ESS used to smooth PV power variations.

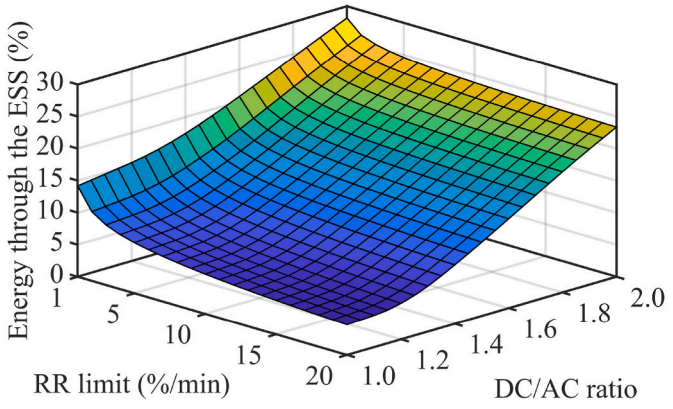

Fig. 14. Share of energy cycled through the ESS as a function of the RR limit and the DC/AC ratio.

4. Discussion

The main objective of this study was to determine the power and energy requirements that PV power variability imposes on the ESSs used for RR control of PV strings, taking into account the effects of the set RR limit and inverter sizing systematically for the first time. Both the power and energy requirements of the ESSs were found to decrease with the increasing RR limit in accord with [33]. The ESS energy capacity needed to smooth all the PV power RRs to comply with the set RR limit increased with the increasing DC/AC ratio, whereas the needed ESS power capacity was quite constant as a function of the DC/AC ratio. These results are in line with [34], in which an ESS was sized for two PV plants with DC/AC ratios of 1.25 and 1.88. The results show that the daily irradiance profile has a crucial effect on the ESS power and energy capacity requirements as expected based on the analysis of PV power fluctuations [4,6,8]. These findings confirm the conclusion of [32] that the local daily PV power production profiles must be considered carefully when sizing the ESSs. The highest ESS charging powers were found to be higher than the highest discharge powers. This is an important finding from the ESS sizing and control points of view. It means that the power ratings of the ESSs can be substantially reduced by smoothing the fastest upward PV power ramps by curtaining the power with the inverter. Since the largest PV power RRs exist only seldom, that would cause only minor power curtailment losses. Naturally, the curtailment losses decrease with increasing RR limit, as reported also in Ref. [34].

Several factors affected the presented results, obviously including the measurement dataset selected. Due to the northern location of our research plant [35], the exact values only represent locations at high latitudes. However, the general findings of the studied phenomena and the conclusions drawn from the obtained results are not regionally bounded but can be applied for sizing of ESSs on a global scale. Moreover, the measurement period affected the obtained results. Use of measurement data of an entire summer would have been an optimal solution. However, that option was not available. Nevertheless, the selected dataset consists of a comprehensive set of days from six summer months including both clear-sky and partially cloudy days. The largest change in measured PV power during 1 s was 39.1% with respect to the nominal MPP power, which is on the same order as the fastest measured rates of change in power observed for three shorter PV strings of the same research plant in Ref. [4]. This indicates that the selected dataset also contains the worst PV fluctuations occurring on this location. The daily irradiance profile has a crucial effect on the ESS power and energy requirements. Thus, the distribution of days with different irradiance conditions affected the obtained results. Therefore, the results were presented as the highest, average and lowest daily values in Figs. 8, 9 and 11. The daily results for all the measurement days are compiled in Table A1, which shows the above.

The starting point for this study was sizing an ESS to compensate for all the PV power fluctuations exceeding the applied RR limit. In that way

the actual power and energy ratings of the ESS imposed by PV power variability could be determined. However, in practice, sizing the ESS to smooth all the PV power fluctuations exceeding the applied RR limit is not economically feasible. Weighing the penalties for failing to meet the set RR limit in extreme power variation cases and balancing the ESS size against benefits in RR mitigation would be an interesting topic for future studies; it has already been touched on in some studies, e.g. in Refs. [34, 37]. Moreover, the varying electricity price affects the economically optimal control strategy of the ESS. The results of Figs. 6 and 12 show that the highest ESS charging powers are higher than the highest discharge powers. Hence, the ESS power rating can be considerably reduced by smoothing the fastest upward power ramps caused by the cloud enhancement phenomenon by curtaining the power just by the inverter instead of feeding all the power to the ESS. Further, the combined use of the ESS with power curtailment, i.e. not cycling all the curtained power though the ESS, combined with the PV power plant DC/AC power ratio is another interesting future research topic.

5. Conclusions

This article presented a comprehensive study on the sizing of ESSs for RR control of PV strings. The effects of RR limit and inverter sizing, including their combined effect, on the sizing of the ESS were studied systematically for the first time. The RR limit was altered from 1 to 20 %/min with respect to the nominal grid connection power and the DC/AC power ratio from 1.0 to 2.0. The study was based on over 2 million *I–U* curves of a PV string of 23 PV modules measured during 38 days in the summers of 2021 and 2022. The starting point for this study was determining the size of the ESS to comply with the set RR limit all the time and in that way determining the power and energy capacities that PV power variability imposes for the ESS. In practice, that kind of sizing is not economically viable, but the ESS should be sized against benefits in RR mitigation. However, the results of this study are valid when the network operator only sets strict RR limits.

The results show that the daily irradiance profile has a crucial effect on the ESS power and energy capacity requirements. On clear-sky days, the ESS is mainly used in preparation for potential power fluctuations, and the maximum energy stored in the ESS is the energy needed to ramp down the highest power fed to the grid in case the PV string is suddenly disconnected. On the other hand, on partly cloudy days with a lot of large power fluctuations, much more capacity is needed for the ESS to smooth all power ramps.

It was found that ESS power capacity of 60% of the PV string nominal power is high enough to smooth nearly all detected PV power ramps even with strict RR limits, while a power capacity rating of 95% is needed to smooth even the fastest PV power ramps that exist only rarely. The highest ESS charging powers were found to be higher than the highest discharge powers, meaning that the ESS power rating can be substantially reduced by smoothing the fastest upward power ramps by curtaining the power with the inverter without storing all the energy in the ESS. Since the fastest power ramps exist only seldom, that would cause only minor power curtailment losses. A typical DC/AC ratio of 1.5 requires an energy capacity of about 1.0 h at the PV string nominal power to smooth all the PV power ramps, while a DC/AC ratio of 2.0 requires about twice the capacity. The results of this study demonstrate that the set RR limit and the inverter sizing should be considered carefully when sizing an ESS for PV power RR control.

CRediT authorship contribution statement

Kari Lappalainen: Conceptualization, Methodology, Formal analysis, Writing – original draft. **Seppo Valkealahti:** Writing – review & editing.

Declaration of competing interest

The authors declare that they have no known competing financial interests or personal relationships that could have appeared to influence the work reported in this paper.

Acknowledgements

The work has received financial support from Business Finland.

Appendix. Daily ESS power and energy ratings

The daily highest charging powers, discharging powers and energies of the ESS for the 38 measurement days together with the daily shares of produced PV energy cycled through the ESS are compiled in Table A1 for an RR limit of 10 %/min and a DC/AC ratio of 1.0.

Table A1
Daily maximum charging powers, discharging powers and energies of the ESS and shares of energy cycled through the ESS for an RR limit of 10 %/min and a DC/AC ratio of 1.0 for all the 38 days.

Day	Maximum $P_{ESS,\ charge}$ (%)	Maximum $P_{ESS,\ discharge}$ (%)	Maximum $E_{ESS}/P_{PV,\ nom}$ (h)	Energy cycled through the ESS (%)
May 7, 2021	7.1	4.3	0.007	1.8
May 8, 2021	74.1	74.6	0.071	6.7
May 9, 2021	57.4	71.9	0.066	7.1
May 10, 2021	5.8	4.2	0.004	2.7
May 11, 2021	21.1	34.5	0.060	3.3
May 12, 2021	4.1	3.0	0.059	0.9
May 25, 2021	31.2	48.1	0.060	3.2
May 26, 2021	44.3	17.4	0.033	4.2
May 28, 2021	90.2	60.4	0.063	17.6
May 29, 2021	15.1	67.6	0.066	1.3
May 30, 2021	5.4	4.6	0.060	0.9
June 4, 2021	59.1	56.9	0.054	4.9
June 5, 2021	54.1	60.6	0.059	3.6
June 6, 2021	46.8	33.6	0.055	4.8
June 7, 2021	69.5	55.2	0.053	4.1
June 8, 2021	70.3	53.3	0.055	9.5
June 9, 2021	66.6	62.7	0.058	10.9
August 6, 2021	31.6	68.9	0.058	3.3
August 7, 2021	68.0	56.4	0.058	12.3

(*continued on next page*)

Table A1 (*continued*)

Day	Maximum $P_{ESS,\ charge}$ (%)	Maximum $P_{ESS,\ discharge}$ (%)	Maximum $E_{ESS}/P_{PV,\ nom}$ (h)	Energy cycled through the ESS (%)
August 8, 2021	64.9	39.6	0.037	6.5
August 9, 2021	84.0	39.7	0.043	11.9
August 10, 2021	69.2	59.5	0.057	14.7
August 11, 2021	59.8	60.7	0.055	10.4
September 3, 2021	86.6	68.2	0.066	17.3
September 4, 2021	82.3	69.3	0.069	12.6
September 5, 2021	27.2	42.7	0.052	4.6
September 6, 2021	47.2	34.3	0.045	6.4
September 7, 2021	16.9	14.3	0.023	2.3
September 8, 2021	49.3	20.0	0.018	7.6
April 23, 2022	61.0	56.6	0.075	7.0
April 24, 2022	58.9	43.8	0.066	2.3
April 25, 2022	10.6	10.9	0.065	1.1
April 26, 2022	70.9	68.5	0.073	5.9
April 27, 2022	78.6	54.7	0.067	9.9
April 28, 2022	15.2	26.9	0.032	4.4
April 29, 2022	65.4	74.3	0.078	6.7
April 30, 2022	82.9	42.2	0.053	7.9
May 1, 2022	78.8	62.4	0.073	6.9
Average	50.8	45.4	0.054	6.6

References

[1] A. Cabrera-Tobar, E. Bullich-Massagué, M. Aragüés-Peñalba, O. Gomis-Bellmunt, Review of advanced grid requirements for the integration of large scale photovoltaic power plants in the transmission system, Renew. Sustain. Energy Rev. 62 (2016) 971–987, https://doi.org/10.1016/j.rser.2016.05.044.

[2] V. Gevorgian, S. Booth, Review of PREPA Technical Requirements for Interconnecting Wind and Solar Generation, National Renewable Energy Laboratory, Golden, CO, USA, 2013. NREL/TP-5D00-57089.

[3] J. Marcos, L. Marroyo, E. Lorenzo, D. Alvira, E. Izco, Power output fluctuations in large scale PV plants: one year observations with one second resolution and a derived analytic model, Prog. Photovoltaics Res. Appl. 19 (2011) 218–227, https://doi.org/10.1002/pip.1016.

[4] K. Lappalainen, S. Valkealahti, Experimental study of the maximum power point characteristics of partially shaded photovoltaic strings, Appl. Energy 301 (2021), 117436, https://doi.org/10.1016/j.apenergy.2021.117436.

[5] S. Shivashankar, S. Mekhilef, H. Mokhlis, M. Karimi, Mitigating methods of power fluctuation of photovoltaic (PV) sources – a review, Renew. Sustain. Energy Rev. 59 (2016) 1170–1184, https://doi.org/10.1016/j.rser.2016.01.059.

[6] K. Lappalainen, S. Valkealahti, Output power variation of different PV array configurations during irradiance transitions caused by moving clouds, Appl. Energy 190 (2017) 902–910, https://doi.org/10.1016/j.apenergy.2017.01.013.

[7] X. Chen, Y. Du, E. Lim, H. Wen, K. Yan, J. Kirtley, Power ramp-rates of utility-scale PV systems under passing clouds: module-level emulation with cloud shadow modeling, Appl. Energy 268 (2020), 114980, https://doi.org/10.1016/j.apenergy.2020.114980.

[8] R. Van Haaren, M. Morjaria, V. Fthenakis, Empirical assessment of short-term variability from utility-scale solar PV plants, Prog. Photovoltaics Res. Appl. 22 (2014) 548–559, https://doi.org/10.1002/pip.2302.

[9] K. Lappalainen, S. Valkealahti, Smoothing of output power variation with increasing PV array size, in: Proceedings of 2018 IEEE Innovative Smart Grid Technologies - Asia Conference, 2018, pp. 190–195, https://doi.org/10.1109/ISGT-Asia.2018.8467900.

[10] J. Marcos, L. Marroyo, E. Lorenzo, D. Alvira, E. Izco, From irradiance to output power fluctuations: the PV plant as a low pass filter, Prog. Photovoltaics Res. Appl. 19 (2011) 505–510, https://doi.org/10.1002/pip.1063.

[11] M. Lave, J. Kleissl, E. Arias-Castro, High-frequency irradiance fluctuations and geographic smoothing, Sol. Energy 86 (2012) 2190–2199, https://doi.org/10.1016/j.solener.2011.06.031.

[12] J. Marcos, L. Marroyo, E. Lorenzo, M. García, Smoothing of PV power fluctuations by geographical dispersion, Prog. Photovoltaics Res. Appl. 20 (2012) 226–237, https://doi.org/10.1002/pip.1127.

[13] G.C. Wang, B. Kurtz, J.L. Bosch, I. de la Parra, J. Kleissl, Maximum expected ramp rates using cloud speed sensor measurements, J. Renew. Sustain. Energy 12 (2020), 056302, https://doi.org/10.1063/5.0021875.

[14] K. Lappalainen, G.C. Wang, J. Kleissl, Estimation of the largest expected photovoltaic power ramp rates, Appl. Energy 278 (2020), 115636, https://doi.org/10.1016/j.apenergy.2020.115636.

[15] M.M. Rahman, A.O. Oni, E. Gemechu, A. Kumar, Assessment of energy storage technologies: a review, Energy Convers. Manag. 223 (2020), 113295, https://doi.org/10.1016/j.enconman.2020.113295.

[16] H.X. Wang, M.A. Munoz-García, G.P. Moreda, M.C. Alonso-García, Optimum inverter sizing of grid-connected photovoltaic systems based on energetic and economic considerations, Renew. Energy 118 (2018) 709–717, https://doi.org/10.1016/j.renene.2017.11.063.

[17] G.A. Rampinelli, A. Krenzinger, F. Chenlo Romero, Mathematical models for efficiency of inverters used in grid connected photovoltaic systems, Renew. Sustain. Energy Rev. 34 (2014) 578–587, https://doi.org/10.1016/j.rser.2014.03.047.

[18] J.M.S. Callegari, A.F. Cupertino, V.N. Ferreira, E.M.S. Brito, V.F. Mendes, H. A. Pereira, Adaptive dc-link voltage control strategy to increase PV inverter lifetime, Microelectron. Reliab. 100–101 (2019), 113439, https://doi.org/10.1016/j.microrel.2019.113439.

[19] J.D. Mondol, Y.G. Yohanis, B. Norton, Optimal sizing of array and inverter for grid-connected photovoltaic systems, Sol. Energy 80 (2006) 1517, https://doi.org/10.1016/j.solener.2006.01.006.

[20] J. Zhu, R. Bründlinger, T. Mühlberger, T.R. Betts, R. Gottschalg, Optimised inverter sizing for photovoltaic systems in high-latitude maritime climates, IET Renew. Power Gener. 5 (2011) 58–66, https://doi.org/10.1049/iet-rpg.2009.0162.

[21] K. Lappalainen, J. Kleissl, Analysis of the cloud enhancement phenomenon and its effects on photovoltaic generators based on cloud speed sensor measurements, J. Renew. Sustain. Energy 12 (2020), 043502, https://doi.org/10.1063/5.0007550.

[22] J. Luoma, J. Kleissl, K. Murray, Optimal inverter sizing considering cloud enhancement, Sol. Energy 86 (2012) 421–429, https://doi.org/10.1016/j.solener.2011.10.012.

[23] K. Lappalainen, S. Valkealahti, Analysis of the operation of PV strings at the MPP closest to the nominal MPP voltage instead of the global MPP based on measured current–voltage curves, EPJ Photovoltaics 13 (2022) 4, https://doi.org/10.1051/epjpv/2022001.

[24] Y. Sun, Z. Zhao, M. Yang, D. Jia, W. Pei, B. Xu, Overview of energy storage in renewable energy power fluctuation mitigation, CSEE Journal of power and energy systems 6 (2020) 160–173, https://doi.org/10.17775/CSEEJPES.2019.01950.

[25] S. Sukumar, M. Marsadek, K.R. Agileswari, H. Mokhlis, Ramp-rate control smoothing methods to control output power fluctuations from solar photovoltaic (PV) sources—a review, J. Energy Storage 20 (2018) 218–229, https://doi.org/10.1016/j.est.2018.09.013.

[26] J. Martins, S. Spataru, D. Sera, D.-I. Stroe, A. Lashab, Comparative study of ramp-rate control algorithms for PV with energy storage systems, Energies 12 (2019) 1342, https://doi.org/10.3390/en12071342.

[27] L. Bridier, D. Hernandez-Torres, M. David, P. Lauret, A heuristic approach for optimal sizing of ESS coupled with intermittent renewable sources systems, Renew. Energy 91 (2016) 155–165, https://doi.org/10.1016/j.renene.2016.01.021.

[28] I. De la Parra, J. Marcos, M. Garcia, L. Marroyo, Control strategies to use the minimum energy storage requirement for PV power ramp-rate control, Sol. Energy 111 (2015) 332–343, https://doi.org/10.1016/j.solener.2014.10.038.

[29] H. Wen, Y. Du, X. Chen, E. Lim, H. Wen, L. Jiang, W. Xiang, Deep learning based multistep solar forecasting for PV ramp-rate control using sky images, IEEE Trans. Ind. Inf. 17 (2021) 1397–1406, https://doi.org/10.1109/TII.2020.2987916.

[30] E. Cirés, J. Marcos, I. de la Parra, M. García, L. Marroyo, The potential of forecasting in reducing the LCOE in PV plants under ramp-rate restrictions, Energy 188 (2019), 116053, https://doi.org/10.1016/j.energy.2019.116053.

[31] S. Sobri, S. Koohi-Kamali, N.A. Rahim, Solar photovoltaic generation forecasting methods: a review, Energy Convers. Manag. 156 (2018) 459–497, https://doi.org/10.1016/j.enconman.2017.11.019.

[32] M. Järvelä, S. Valkealahti, Comparison of AC and DC bus interconnections of energy storage systems in PV power plants with oversized PV generator, in: Proceedings of 2019 IEEE 46th Photovoltaic Specialists Conference, 2019, pp. 2956–2961, https://doi.org/10.1109/PVSC40753.2019.8980909.

[33] J. Marcos, O. Storkël, L. Marroyo, M. Garcia, E. Lorenzo, Storage requirements for PV power ramp-rate control, Sol. Energy 99 (2014) 28–35, https://doi.org/10.1016/j.solener.2013.10.037.

[34] A. Makibar, L. Narvarte, E. Lorenzo, Contributions to the size reduction of a battery used for PV power ramp rate control, Sol. Energy 230 (2021) 435–448, https://doi.org/10.1016/j.solener.2021.10.047.
[35] D. Torres Lobera, A. Mäki, J. Huusari, K. Lappalainen, T. Suntio, S. Valkealahti, Operation of TUT solar PV power station research plant under partial shading caused by snow and buildings, Int. J. Photoenergy 2013 (2013), 837310, https://doi.org/10.1155/2013/837310.
[36] H. Shin, J.H. Roh, Framework for sizing of energy storage system supplementing photovoltaic generation in consideration of battery degradation, IEEE Access 8 (2020) 60246–60258, https://doi.org/10.1109/ACCESS.2020.2977985.
[37] A. Makibar, L. Narvarte, E. Lorenzo, On the relation between battery size and PV power ramp rate limitation, Sol. Energy 142 (2017) 182–193, https://doi.org/10.1016/j.solener.2016.11.039.